Early View publication on wileyonlinelibrary.com
(issue and page numbers not yet assigned;
citable using Digital Object Identifier – **DOI**)

Phys. Status Solidi C, 1–4 (2011) / **DOI** 10.1002/pssc.201000850

physica status solidi c
www.pss-c.com
current topics in solid state physics

InAs quantum dot site-selective growth on GaAs substrates

Joshua Hendrickson[*,1], Mathieu Helfrich[2,3], Michael Gehl[1], Dongzhi Hu[3], Daniel Schaadt[2,3], Stefan Linden[4], Martin Wegener[2,3], Benjamin Richards[1], Hyatt Gibbs[1], and Galina Khitrova[1]

[1] College of Optical Sciences, University of Arizona, 1630 E. University Blvd, Tucson, AZ 85721, USA
[2] Institute of Applied Physics, Karlsruhe Institute of Technology (KIT), Wolfgang-Gaede-Straβe 1, 76131 Karlsruhe, Germany
[3] DFG-Center for Functional Nanostructures (CFN), Karlsruhe Institute of Technology (KIT), Wolfgang-Gaede-Straβe 1, 76131 Karlsruhe, Germany
[4] Institute of Physics, University of Bonn, Nuβallee 12, 53115 Bonn, Germany

Received 13 August 2010, revised 14 October 2010, accepted 15 October 2010
Published online 1 February 2011

Keywords quantum dot, MBE, deterministic growth, annealing

* Corresponding author: e-mail jhendrickson@optics.arizona.edu

Photoluminescence (PL) spectra and AFM measurements of InAs quantum dots grown in a site-selective manner on pre-patterned GaAs substrates are presented. A number of processing steps are described including a Ga-assisted deoxidation step to remove native oxides from the sample surface. Furthermore, post growth annealing is shown to be a promising technique for improving the quantum dot density and likelihood of single site-selective nucleation. Morphological transitions are shown to occur during the annealing process with two initial quantum dots in a given nucleation site transforming into one slightly larger quantum dot. Density measurements performed by AFM combined with PL spectroscopic measurements show that we have achieved optically active, site-selective dot growth, and additionally allow us to calculate that our site-selective dots are on average 30% as efficient as unpatterned dots.

1 Introduction Semiconductor quantum dots have been shown to exhibit a number of interesting and useful properties such as photon antibunching [1], resonance fluorescence [2], and generation of entangled photon pairs [3]. This makes them an increasingly popular choice of emitter for single photon sources and quantum information/quantum cryptography devices. Through the coupling of semiconductor quantum dots to various types of cavities even the strong coupling regime of cavity quantum electrodynamics can be reached [4-6]. However, the inherent randomness in the spatial distribution of self-assembled quantum dots grown in the Stranski-Krastanov growth mode makes it difficult to align quantum dots to cavities, waveguides, or any other structures. Often one may simply rely on luck to obtain the correct spatial positioning. Some groups have devised methods of locating a particular quantum dot and then fabricating a device around it [7-9]; however, these are not very scalable methods. To circumvent such problems we have been working towards the deterministic, site-selective growth of quantum dots [10] on pre-patterned substrates.

The method we have chosen for producing site-selective nucleation of semiconductor quantum dots is through the creation of small nanoholes on the substrate surface. Using electron beam lithography and wet chemical etching, arrays of nanoholes having average diameters of 60 nm and AFM measured depths of 20 nm are produced. After cleaning the samples chemically they are reintroduced into the MBE chamber where they undergo a Ga-assisted deoxidation process [11] for the removal of native oxides. Next, the growth of InAs quantum dots occurs followed by an *in-situ* annealing step to help reduce defects, control dot size and density, and increase the probability of single dot nucleation at each pre-defined location. Finally the sample may or may not be capped with GaAs depending upon whether photoluminescence measurements or atomic force microscopy measurements are to be taken.

2 Experimental details

2.1 Nanohole fabrication The fabrication of the nanoholes which will later serve as the nucleation sites

during quantum dot growth is carried out by first spin coating a layer of PMMA/MA (polymethyl methacrylate/methacrylate) onto a GaAs substrate. Several square arrays of spots with various lattice spacing are then written into the resist by electron beam lithography (Raith e-line, 30 keV). After developing the resist the sample is placed in a solution of H_2SO_4:H_2O_2:H_2O (1:8:800) for 30 s in order to wet chemically etch holes of depth 20 nm into the substrate.

2.2 Sample cleaning The first step in the cleaning process is to remove the remaining resist. This is accomplished through a series of solvent baths including acetone, methanol, and isopropyl alcohol. The sample is then placed into the load lock chamber of a Riber Compact 21T molecular beam epitaxy system where it is held for 1 hour at 130°C in order to desorb any volatile surface contamination. The final cleaning step involves the removal of surface oxides by an *in-situ* Ga-assisted deoxidation process where the sample is heated up to 480 °C and then exposed to a low Ga flux of 1 ML/s. The exposure of Ga is cycled repeatedly for 30 seconds on and 30 seconds off with the As shutter always closed, giving the converted Ga_2O time to desorb from the sample surface. Once the total amount of Ga provided reaches 8 ML the cycling is stopped and the sample temperature is increased to 550 °C and annealed for 2 minutes under As_4 atmosphere to thermally desorb any remaining oxide compounds.

2.3 Quantum dot growth The InAs quantum dot growth process begins with the growth of a 16 nm GaAs buffer layer at 500 °C followed by 1.7 ML of InAs. Using III/V beam equivalent pressure ratios of 1:10 and 1:100, the GaAs and InAs growth rates were determined to be 0.3 ML/s and 0.07 ML/s, respectively. An *in-situ* annealing step is performed immediately after quantum dot growth with the sample being kept at growth temperature for 2:30 min. Afterwards the sample is either rapidly cooled down to room temperature or capped with 80 nm of GaAs. Uncapped samples are used in atomic force microscopy (AFM) measurements in order to determine quantum dot size, density, and distribution while the capped samples are used in photoluminescence measurements in order to discern their optical quality.

3 Results and discussion

3.1 AFM measurements The electron beam lithography and wet chemical etching are able to reliably produce nanoholes with diameters in the range of about 60 nm. Fig. 1 shows an AFM image of the nanoholes, before quantum dot growth. The holes actually appear to be more rectangular then circular due to selective etching of the [111] GaAs sidewall and elongation along the [011] direction. Average hole size was measured as 58.4±6.1 nm.

In Fig. 2 AFM images are shown for two samples where all growth and fabrication parameters were kept constant with the exception of the annealing step. Quantum dot growth is preferentially located at each nucleation site for both samples. The unannealed sample shows a predominance of double dot nucleation at each site. This double dot growth feature is expected to arise from the change in nanohole shape during buffer layer growth [12]. As the buffer layer thickness increases the holes become both wider and shallower and may eventually split into two separate holes, thus increasing the probability of double dot nucleation. The average diameter of the unannealed dots is 49.1±4.4 nm, and the average height is 7.4±0.9 nm.

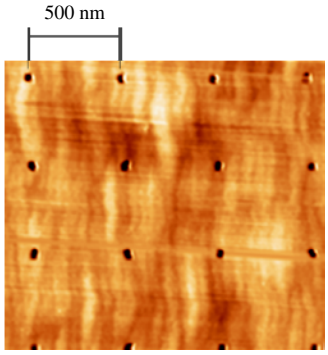

Figure 1 AFM image of nanoholes, before quantum dot growth.

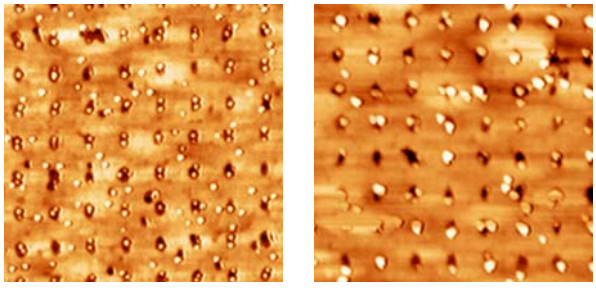

Figure 2 AFM images comparing as grown (left) sample A1083 with annealed (right) sample A1085.

Upon performing the 2:30 minute *in-situ* annealing step, a morphological change in the quantum dots occurs with formerly double dots now transforming into single dots as a consequence of the migration of adatoms. The size of the annealed dots has become larger than those grown without the annealing step, with an average diameter of 82.6±9.5 nm. The size should be controllable by increasing the annealing time which should result in a loss of material resulting in smaller quantum dot size. It is also of interest to note that the number of between-hole quantum dots is decreased from ~45% down to ~30% during the annealing process. This implies that deterministic, site-selectively grown quantum dots are more stable than between-hole quantum dots; indium is preferentially removed from dots between holes and redistributed to the site-selective quantum dots.

There are a number of steps within the process of growing site-selective quantum dots that can adversely

affect the outcome. Remnant resist and surface oxide can result in defect holes appearing within the nanohole array. Quantum dot growth must be optimized, along with annealing time, in order to decrease the probability of quantum dot growth between holes. This optimization procedure is still in progress.

3.2 Photoluminescence measurements In addition to growing quantum dots of the correct size and locating them where one wishes, it is also important that the quantum dots are of high enough optical quality to be useful as an emitter. In order to assess the optical quality of the quantum dots, photoluminescence (PL) measurements are performed. The samples of interest are placed into a continuous flow liquid helium cryostat and cooled down to 10 K. A pair of x-y nanopositioners is located within the cryostat, allowing for access to different regions of the sample such as patterned areas with different lattice spacing or unpatterned areas for making comparison measurements. The samples are pumped above band by a HeNe laser beam at 632.8 nm, and the quantum dot emission is collected in reflection geometry using a 100x objective. The PL is then dispersed with a 1.26 m spectrometer and detected with a liquid nitrogen cooled silicon CCD.

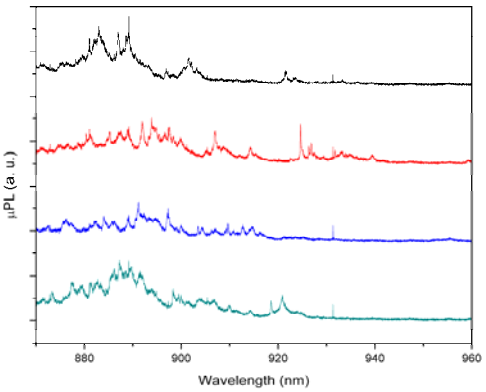

Figure 3 Spectra at four different locations in the unpatterned area of sample A1078 (vertically offset for clarity).

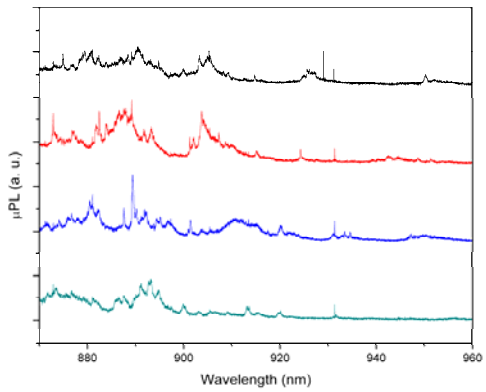

Figure 4 Spectra at four different locations in the patterned area of sample A1078 (vertically offset for clarity).

PL spectra taken at four different locations within the unpatterned (patterned area) of a sample containing a lattice spacing of 250 nm are presented in Fig. 3 (Fig 4). Single quantum dot emission lines can be observed in the spectra with linewidths as narrow as 180 μeV. The spatial resolution of the PL detection is about 1 μm, so it is not possible to distinguish a dot grown in a hole from one grown between holes. Nonetheless, there is statistical evidence that quantum dots grown in holes are emitting PL. Two AFM 5 μm by 5 μm scans of uncapped sample A1083 revealed 746 and 696 quantum dots in an unpatterned region; similarly, on a nearby patterned region with pitch 250 nm, 441 and 484 dots were found between holes and 577 and 576 inside holes. PL data were taken on capped sample A1078 with dots otherwise grown identically as shown in Figs. 3 and 4; integrating the spectra (accounting for detector spectral response) yields $5.15{\cdot}10^5$ counts/mW from the unpatterned region and $4.54{\cdot}10^5$ counts/mW from the patterned region. If quantum dots between holes emit as efficiently as dots in the unpatterned region, then one would expect between-hole dots to emit a PL signal in the ratio of the average number of quantum dots times the unpatterned region PL: $[\{(441 + 484)/2\}/\{(746 + 696)/2\}](5.15{\cdot}10^5$ counts/mW) $= 3.3{\cdot}10^5$ counts/mW. Since the PL coming from the patterned region ($4.54{\times}10^5$ counts/mW) exceeds this number by 38%, the extra light must come from quantum dots grown in the holes.

One can extract an effective quantum efficiency η_{in} (η_{bet}) for quantum dots in holes (between holes) in the patterned region as follows. We also took data as above on the same sample for 500 nm pitch, finding an average number of quantum dots between holes of $N_{bet} = 771.5$, in holes of $N_{in} = 36.5$, and integrated PL spectrum of $PL_{500} = 5.57{\cdot}10^5$ counts/mW. Using $C{\cdot}PL_{500} = \eta_{bet}N_{bet} + \eta_{in}N_{in}$, where C is a proportionality constant, and a similar formula for PL_{250}, we calculate $\eta_{in}/\eta_{bet} = 0.306$. Then from one of these equations and one for the unpatterned region, namely $C{\cdot}PL_{unpatt} = \eta_{unpatt}N_{unpatt}$, one finds $\eta_{bet}/\eta_{unpatt} = 0.996$. These results show that the effective quantum efficiency for dots grown between holes in the patterned region is essentially the same as for dots grown in the unpatterned region, and that the average effective quantum efficiency for dots grown in holes is 30.6% that for dots grown between holes. This method gives us a quantitative measure to evaluate changes we make in electron-beam lithography, etching, cleaning, buffer and quantum dot growth, etc. in an effort to reach our goal of $\eta_{in} = 1$.

These are preliminary results that will be repeated and optimized to increase the ratio of dots in holes to between-hole dots, to increase the PL quantum efficiency, and to reduce the size of the dots as discussed below. However, these results are highly encouraging that dots grown in pre-etched holes are of high enough quality to emit light.

In addition to being of high optical quality it is also of importance that the quantum dots be truly quantum in

nature; i.e. their photon statistics should display antibunching. The annealing process used here resulted in quantum dots with diameters in the range of 70-90 nm. It is questionable whether or not the second order correlation function for quantum dots of this size will show antibunching. While we have not performed this measurement yet it will be pursued in the future. Furthermore, adjustments in both the annealing process [13] and the amount of deposited InAs should allow for reduction in quantum dot size.

4 Conclusion In conclusion, the site-selective growth of arrays of optically active quantum dots has been demonstrated. An *in-situ* annealing process has been utilized, transforming most double quantum dots into single quantum dots through migration of adatoms and quantum dot ripening, therefore reducing the dot density. Annealing also reduces the number of between-hole quantum dots while maintaining or improving the number of site-selective quantum dots. This implies the site-selective dots are quite stable. Finally, photoluminescence measurements, though not yet spatially resolving an individual site-selective quantum dot, demonstrate statistically that light is emitted by at least some of the site-selective dots.

Acknowledgements The Tucson group would like to acknowledge financial support from the National Science Foundation through the Engineering Research Center for Integrated Access Networks (EEC-0812072), Atomic Molecular and Optical Physics, and Electronics, Photonics and Device Technologies, as well as AFOSR and Arizona Technology & Research Initiative Funding. The Karlsruhe researchers acknowledge support from the Deutsche Forschungsgemeinschaft (DFG) and the State of Baden-Württemberg through the DFG-Center for Functional Nanostructures (CFN) within subproject A2.6.

References

[1] C. Santori, M. Pelton, G. Solomon, Y. Dale, and Y. Yamamoto, Phys. Rev. Lett. **86**, 1502 (2001).
[2] A. Muller et al.,Phys. Rev. Lett. **99**, 187402 (2007).
[3] N. Akopian et al., Phys. Rev. Lett. **96**, 130501 (2006).
[4] T. Yoshie et al., Nature **432**, 200 (2004).
[5] J. P. Reithmaier et al., Nature **432**, 197 (2004).
[6] A. Badolato et al., Science **308**, 1158 (2005).
[7] G. Khitrova, H. M. Gibbs, M. Kira, S. W. Koch, and A. Scherer, Nat. Phys. **2**, 81 (2006).
[8] A. Dousse et al., Phys. Rev. Lett. **101**, 267404 (2008).
[9] S. M. Thon et al., Appl. Phys. Lett. **94**, 111115 (2009).
[10] O. G. Schmidt et al., Surf. Sc. **514**, 10 (2002).
[11] P. Atkinson, S. Kiravittaya, M. Benyoucef, A. Rastelli, and O. G. Schmidt, Appl. Phys. Lett. **93**, 101908 (2008).
[12] S. Kiravittaya, H. Heidemeyer, and O. G. Schmidt, In(Ga)As Quantum Dot Crystals on Patterned GaAs(001) Substrates, in: Lateral Alignment of Epitaxial Quantum Dots, edited by O. G. Schmidt (Springer, 2007).
[13] D. Z. Hu, A. Trampert, and D. M. Schaadt, J. Cryst. Growth **312**, 447 (2010).

